Journal of
Marine Science and Engineering

MDPI

Article

Why Do Bio-Carbonates Exist?

Luis Pomar [1], Pamela Hallock [2,*], Guillem Mateu-Vicens [3] and Juan I. Baceta [4]

[1] Catedra Guillem Colom, Universitat de les Illes Balears, E-07122 Palma de Mallorca, Spain
[2] College of Marine Science, University of South Florida, St. Petersburg, FL 33701, USA
[3] Department of Biology, Universitat de les Illes Balears, E-07122 Palma de Mallorca, Spain
[4] Department of Geology, University of the Basque Country UPV-EHU, E-48940 Leioa, Spain
* Correspondence: pmuller@usf.edu

Abstract: Calcium carbonate precipitation associated with biotic activity is first recorded in Archaean rocks. The oldest putative fossils related to hydrothermal vents have been dated at ~3.77 Ga (possibly 4.29 Ga). Stromatolites, the oldest dated at 3.70 Ga, have since occurred through Earth history, despite dramatic changes in physical and chemical conditions in aquatic environments. A key question is: what advantages do photosynthesizing aquatic prokaryotes and algae gain by precipitating carbonates? We propose the Phosphate Extraction Mechanism (PEM) to explain the benefits of biomineralization in warm, oligotrophic, alkaline, euphotic environments. Carbonate precipitation enhances access to otherwise limited carbon dioxide and phosphate in such environments. This mechanism also provides an explanation for prolific production of carbonates during times of elevated atmospheric carbon dioxide at intervals in the Phanerozoic.

Keywords: phosphate; nutrient limitation; carbon dioxide; Archaean; Proterozoic; cyanobacteria; calcareous algae; coccolithophores

Citation: Pomar, L.; Hallock, P.; Mateu-Vicens, G.; Baceta, J.I. Why Do Bio-Carbonates Exist?. *J. Mar. Sci. Eng.* **2022**, *10*, 1648. https://doi.org/10.3390/jmse10111648

Academic Editors: Hildegard Westphal, Justin Ries and Steve Doo

Received: 27 September 2022
Accepted: 21 October 2022
Published: 3 November 2022

Publisher's Note: MDPI stays neutral with regard to jurisdictional claims in published maps and institutional affiliations.

1. Introduction

Carbon (C), which is the major component of fossil fuels [1], is the key ingredient in "life" [2]. Carbon is also a key ingredient in limestones ($CaCO_3$) and other carbonate rocks [3]. The ultimate sources of carbon are the primordial components of the Earth [2]. Even at present, volcanic sources emit ~6×10^8 metric tons of carbon dioxide (CO_2) per year [4]. Through geologic history, the dynamics of carbon chemistry have played major roles in oceanic, terrestrial and even subsurface-crustal processes [2]. Human activities are now contributing roughly 40 billion tons of CO_2 annually into the Earth's atmosphere [5], with climatic consequences that are becoming more apparent every year.

The systematic measure of CO_2 concentrations in the atmosphere was started by C. David Keeling of the Scripps Institution of Oceanography in March 1958 at a NOAA (National Oceanic and Atmospheric Administration) facility at Mauna Loa Observatory, Hawai'i, USA [6]. NOAA initiated its own CO_2 measurement in May 1974 and, since then, NOAA and Scripps have run the measurements in parallel [7]. Prior to Keeling's research, CO_2 measurements were inconsistent, but the Keeling's methods revealed a pattern of seasonal oscillations of CO_2, with peaks in May and lows in November, with the averaged values of successive years progressively increasing (Figure 1). Keeling envisaged the yearly cycles to reflect the vegetation cycles that prevail across the northern hemisphere while the increase over time was thought to be caused by human activities, especially the burning of fossil fuels [8].

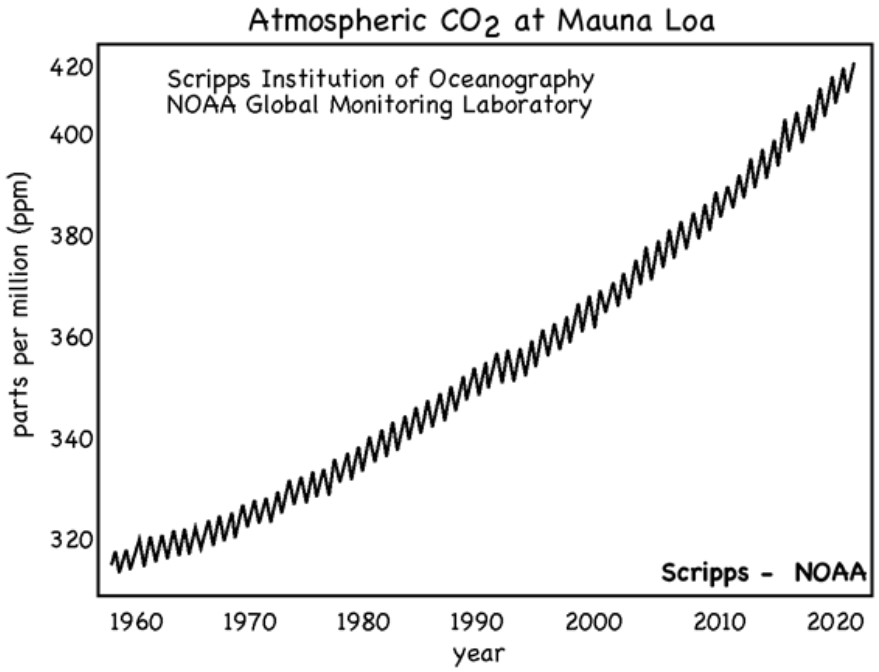

Figure 1. CO_2 concentrations in the atmosphere [7], started by C. David Keeling of the Scripps Institution of Oceanography in March 1958 [8]. (Adapted with permission from Scripps CO_2 program, Scripps Institution of Oceanography at UC San Diego, CA, USA.).

By the 1960's, greenhouse gas emissions and their link to global climate change became a serious concern, with both scientists and the public considering CO_2 to be an invisible pollutant. Attention and concern for greenhouse gases and their role in climate change intensified, and in 1988 the United Nations created the Intergovernmental Panel on Climate Change (IPCC) [9]. Concern for ocean acidification, *climate change's equally evil twin*, emerged somewhat later. Although scientists had been tracking ocean pH for more than 30 years, biological studies emerged in the 1990s [10] and have accelerated since the introduction of the term "ocean acidification" in 2003 [11].

Burning of fossil fuels, combined with widespread changes in land use, has resulted in rapidly increasing concentrations of atmospheric CO_2 that are causing the decline in the pH of surface seawater [10–14]. Will progressive warming and acidification cause mass extinctions and evolutionary turnover of marine biotas, as occurred at previous events that caused major perturbations of ocean chemistry [15–17]?

This question reveals a major paradox in the geologic record. Through the Phanerozoic, extended Greenhouse World times of higher CO_2 (Silurian–Devonian and Jurassic–Cretaceous) were characterized by prolific accumulations of biogenic carbonates, especially those associated with cyanobacterial and algal calcification (Figure 2).

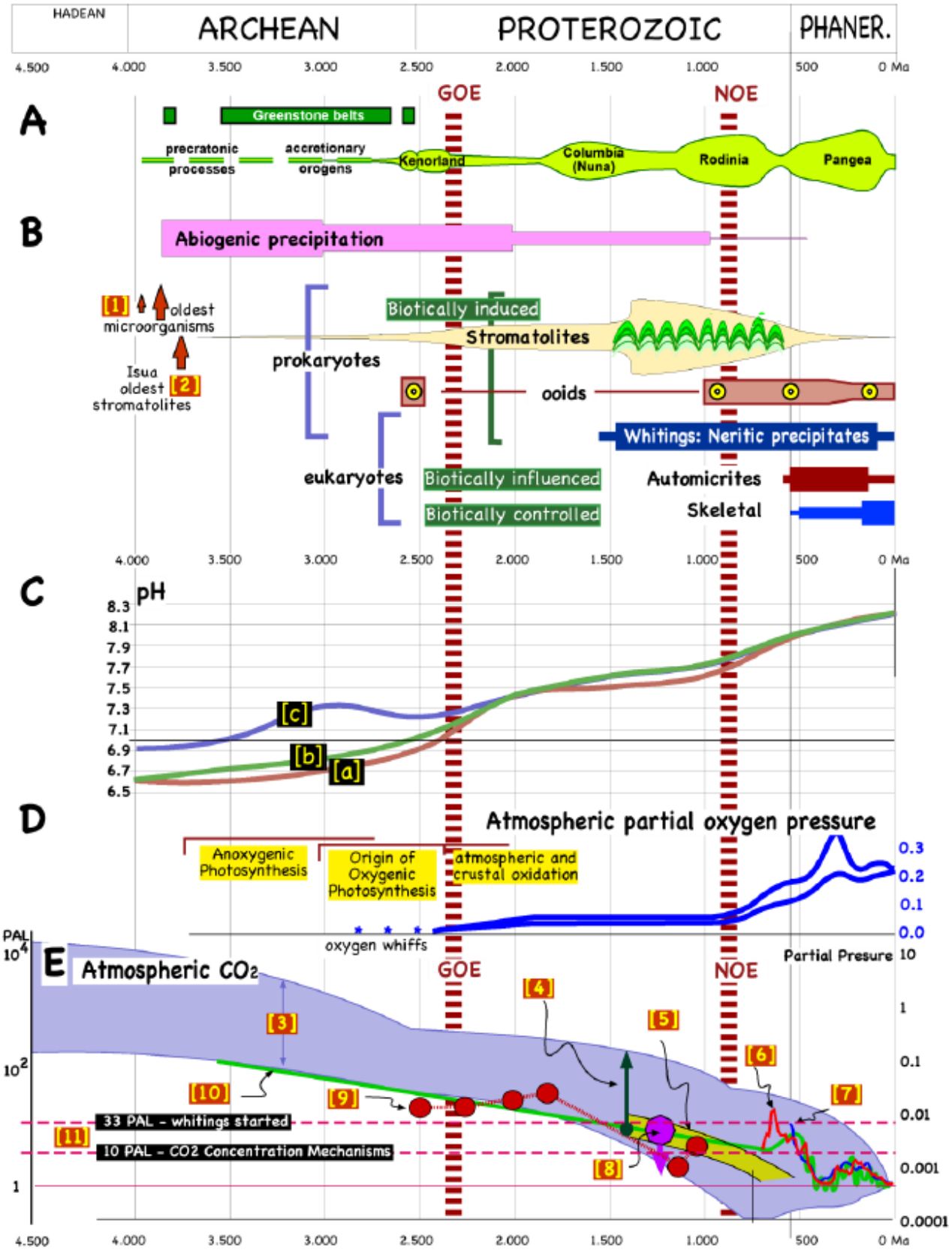

Figure 2. Carbonate precipitation nodes, genetic macroevolution rates, and estimates of oxygen and CO_2 in the atmosphere. (**A**): Supercontinents and crustal growth; precratonic, accretionary orogens and supercontinents assembly (redrawn from multiple sources). (**B**): Carbonate precipitation modes

through Earth's history (multiple sources). [1]: Oldest fossils [18]. [2]: Isua oldest stromatolites [19]. (**C**): pH evolution from [20]; [**a**]: nominal model, in which the median Archean surface temperature is slightly higher than modern surface temperatures. Archean land fraction was anywhere between 10% and 75% of modern land fraction; [**b**]: no Archean land endmember scenario; [**c**]: model with assumed 100 ppm Proterozoic methane and 1% Archean methane levels. (**D**): Maximum and minimum estimates of atmospheric partial oxygen pressure (after [21]). (**E**): Estimates of atmospheric CO_2 concentration; [3] from [22], upper and lower boundaries reflect average surface temperature for an ice-free (20 °C) and ice covered (5°) Earth; [4] Acritarch isotopic composition [23]; [5] C-isotope reservoir modeling [24]; [6] Phanerozoic GEOCARB III models [25]; [7] Royer compilation [26]; [8] from [27]; [9] paleosoil mass balances [28]; [10] from [29]; [11] Picoplanktonic whiting and partial sheath calcification commenced 1400–1300 Ma ago (33 CO_2 PAL), and cyanobacteria CCMs were induced when pCO_2 = 10 PAL [30]. PAL: present atmospheric level; GOE: the Great Oxygenation Event; NOE: Neoproterozoic oxygenation event. (This figure is an original compilation and interpretation of data by L. Pomar, based upon numerous sources).

For example, during the Cretaceous, micritic and algal (e.g., coccoliths) production was prolific. The emergence of rudists as major metazoan producers of skeletal carbonates was notable, and the "elevator" nature of many lineges has been postulated to have been the response to rapid inundation by carbonate muds. In the Cenozoic, the Paleogene was a time of transition. Coccolithophores and planktic foraminifers emerged as major producers of pelagic carbonate sediments through the Mesozoic. Following the Cretaceous-Paleogene extinction, new lineages of coccolithophores and planktic foraminifers diversified, while calcareous macroalgae and larger benthic foraminifers were notable producers of neritic carbonates. Coral reefs emerged as major carbonate factories as Icehouse World conditions developed in the Oligocene and became predominant in the Neogene, a conundrum noted more than 45 years ago [31].

Another paradox associated with changes in ocean chemistry over the course of Earth history relates to another essential element for life, which is commonly the most limiting nutrient required for essential processes including photosynthesis, growth and reproduction. Bioavailable phosphorus (P), typically occurring as phosphate (PO_4^{3-}), provides the backbone of nucleotides (DNA and RNA) and phospholipid membranes of cells, and is used in many other essential functions including energy storage and transfer associated with adenosine triphosphate (ATP), and for the synthesis of proteins and enzymes. Kempe and Degens [32] postulated that abundant dissolved PO_4^{3-} in the Archaean seas helped to foster the evolution of life (see also [33,34]).

2. The Hypothesis

The goal of our paper is to explore the hypothesis that decline in both CO_2 and PO_4^{3-}, and the history of changes in modes of calcification through Earth history, are tied to the close and complex relationships between biogenic carbonates and phosphate availability. The **Phosphate Extraction Mechanism** (**PEM**) provides an explanation for how calcifying microbial and algal biota can thrive in oligotrophic conditions. During daylight, calcification can be coupled to photosynthesis. With energy from active ion transport, protons can be split from bicarbonate, providing a carbonate ion (CO_3^{2-}) for calcification and a CO_2 molecule for photosynthesis. Phosphate is adsorbed during calcium carbonate ($CaCO_3$) precipitation. At night, respiration releases CO_2 and can promote partial dissolution of diurnally precipitated carbonates. Phosphate that is adsorbed onto precipitating $CaCO_3$ during daylight can be desorbed at night, making it available for uptake by the calcifying cyanobacteria or algae.

3. The Hadean–Archaean

Conditions on the Hadean Earth were clearly very different from present, and even from those of the Proterozoic. One hypothesis is that the early Earth was hot, following the

moon-forming impact, and cooled to the point where liquid water was present after about 10 million years [35,36]. Whether the Earth's surface continued to be thermophilic well into the Archaean is still debated, though ~4.3 Ga rocks near Hudson Bay are suspected to have formed under warm, greenhouse conditions [37].

Over the past 4.5 Ga, heat-, gravity-, and tectonically driven processes have concentrated Iron (Fe) and Nickel (Ni) in the Earth's core. The dominant elements in the Earth's crust are Oxygen (O), Silicon (Si), Aluminum (Al), Iron (Fe), Calcium (Ca), Magnesium (Mg), Sodium (Na), and Potassium (K). In the mantle, Mg is nearly an order of magnitude more prevalent than in the crust, where proportions especially of Si and Al are higher. Basaltic, komatiitic (ultramafic) and mantle ejecta are potent CO_2 sinks (all are rich in Mg^{2+} and Fe^{2+}, with somewhat less Ca^{2+}) and their subduction may have drawn down atmospheric CO_2 [36,38]. Alkalic rocks in India indicate carbonate subduction occurred by 4.26 Ga [36].

Through the Archaean, the combination of high atmospheric CO_2 concentrations and the prevalence of Mg^{2+}, Fe^{2+}, and Ca^{2+} resulted in formation of massive abiogenic dolomites and limestones, indicating extreme oversaturation of waters [39] (Figure 2B). The earliest hints of life date back ~3.8 billion years (early–mid Archaean, Figure 2A,B), and by ~3.7 Ga, some metacarbonate rocks, found in the Isua supercrustal belt in southwest Greenland, contain 1–4-cm-high isolated and aggregated stromatolites [19]. Through the Proterozoic, massive abiogenic carbonates declined in prevalence relative to biogenic carbonates and are unknown in modern marine environments, even in those that are strongly oversaturated with respect to $CaCO_3$. In a water body containing abundant Ca^{2+} and dissolved inorganic carbon, modest increases in saturation, whether by warming, reduced hydrostatic pressure, evaporation, or by biogenic processes such as photosynthetic uptake of CO_2 or microbial sulfate reduction, can trigger $CaCO_3$ or $CaMg(CO_3)_2$ precipitation.

So the questions we pose are these: In post Archaean oceans, did biogenic processes become so ubiquitous that they became the drivers and controllers of $CaCO_3$ precipitation, resulting in the overwhelming predominance of biogenic carbonate production? Was the sequence of carbonate factories through geologic history, from predominantly abiogenic precipitation in the Archaean, to predominance of biologically induced geochemical precipitation in the Proterozoic, to the addition of biologically controlled calcification during the Phanerozoic (Figure 2B), consistent with and driven by evolutionary processes involving luminosity of the Sun, the stratification of the Earth, and the emergence of life, with their combined effects on ocean chemistry (Figure 2C)?

The luminosity of the Sun has increased ~30% during the past 4.5 Ga [40]. The composition of the Earth's atmosphere has changed (Figure 2D,E), with substantial decline in greenhouse gases, including CO_2 (Figure 2E) and methane (CH_4). For example, CO_2 has been estimated to have been ~100 times higher in the Hadean than modern levels and ~10 times higher in the Cambrian than present [36]. As noted above, ultramafic ejecta are potent CO_2 sinks and their subduction may have drawn down atmospheric CO_2 in the Hadean [38].

4. Pertinent Chemical Processes

Before delving into biological processes, we briefly examine some chemical factors associated with CO_2 in aqueous environments (Figure 3). Two measures associated with but not restricted to CO_2 are pH and alkalinity. Both are important in water chemistry, but their interactions can be confusing when considering calcification (29,38,41). The concentration of hydrogen ions (H^+), indicating how acidic or basic a substance is, is measured as pH. Alkalinity indicates the ability of a solution to neutralize acids (i.e., buffering capacity). Alkalinity consists of ions that can incorporate H^+ (protons) into their structure, limiting the availability of those protons that would otherwise lower pH. Carbonate alkalinity measures the concentrations of CO_3^{2-} and HCO_3^- ions, which are typically present in the highest concentrations in natural waters. Total Alkalinity reflects primarily CO_3^{2-} and HCO_3^- ions, but also includes PO_4^{3-}, borate, orthosilicate, sulfides, and organic acids.

Shallow water bodies can be strongly influenced by rising temperature and evaporation, concentrating the alkaline ions and promoting the precipitation of carbonate minerals, assuming that appropriate cations are available (e.g., Ca^{2+}, Mg^{2+}). Moreover, any process that takes up protons can also promote such precipitation.

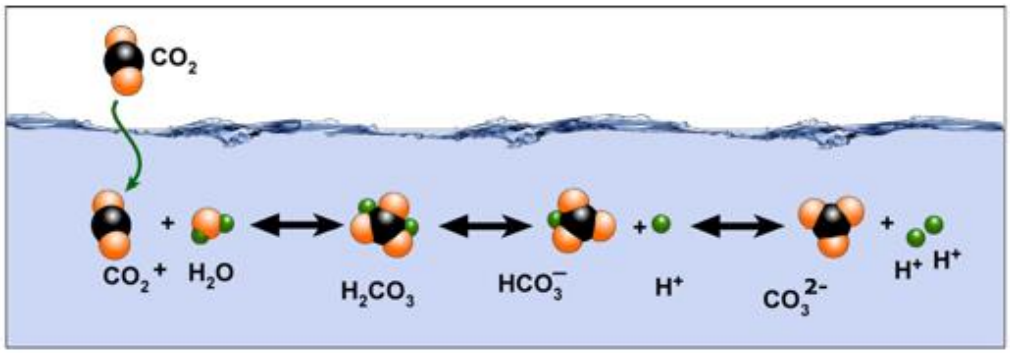

Figure 3. In an aqueous solution, carbonate, bicarbonate, carbon dioxide, and carbonic acid exist together in dynamic equilibrium, e.g., [10,20]. When CO_2 is absorbed by seawater, a series of chemical reactions increase the concentration of H^+ and cause the seawater acidity to increase. When calcium carbonate (e.g., limestone) reacts with acidic free hydrogen (H^+) ions in seawater, the solid calcium carbonate dissolves, releasing free calcium (Ca^{2+}) ions and free bicarbonate (HCO_3^-) ions. (This figure is an original interpretation by L. Pomar based on numerous sources).

As elements that are relatively abundant in both crustal and mantle rocks, Mg^{2+}, Fe^{2+}, and Ca^{2+} ions are soluble in aquatic environments. Thus, the combination of high carbonate alkalinity and abundant reactive cations, especially in warm waters, provided prolific sources of ions to produce abiogenic carbonates, providing critical storage of atmospheric CO_2 on geological time scales [41].

5. Pertinent Biological Processes

All living organisms carry traces of the histories of their ancestors within their genetic makeup and, in the case of the Eukarya, literally within their cells. The diversity of metabolic pathways in the prokaryotic Archaea and Eubacteria far surpasses the comparatively limited pathways found in the Eukarya, which are metabolically limited to those of their Proteoarchaeota and α-proteobacterial symbiotic predecessors [42].

Early microbial forms evolved in aquatic environments lacking free oxygen (O_2). Autotrophic processes in aquatic systems require: (a) an energy source, (b) source of dissolved inorganic carbon (DIC), (c) a source of protons, and (d) nutrients (fixed N, P, Fe, and trace elements) necessary for cell growth and reproduction [43]. Energy sources include oxidation of inorganic compounds (e.g., H_2S, CH_4) by chemoautotrophs and sunlight by photoautotrophs [44]. The primary sources of DIC are CO_2 or CH_4. In photoautotrophy, proton donors can be H_2, Fe^{2+} or H_2S, which do not release O_2 (anoxygenic photosynthesis), or H_2O that releases O_2 as a byproduct (oxygenic photosynthesis).

RuBisCO is the enzyme that catalyzes the first major step of carbon fixation in the Calvin cycle, the process of photosynthesis. As the most abundant protein on Earth, RuBisCO is found in all three domains of life (Eubacteria, Archaea and Eukarya), and fixes more than 90% of the inorganic carbon that is converted into biomass [45]. However, this enzyme evolved in an O_2-free atmosphere, prior to the Great Oxygenation Event, and does not efficiently discriminate between CO_2 and O_2. Enzyme activity and specificity are reciprocally linked: faster RuBisCO has a higher error rate and more specific RuBisCO has a lower catalytic rate [45].

6. CCMs: CO_2 Concentrating Mechanisms

It may seem paradoxical that RuBisCO, this ubiquitous and essential enzyme, has not become more efficient or been replaced by more efficient enzymes. However, CCMs (CO_2 concentrating mechanisms) evolved instead by adaptation of active transport processes and compartmentalization of accumulated HCO_3^- [46]. The CCMs in cyanobacteria and microalgae enhance photosynthetic carbon fixation by energy-driven uptake of HCO_3^- and its conversion to CO_2. The minimum requirements for a cyanobacterial CCM are one energy-driven active transporter that accumulates HCO_3^- in the cytosol, and an anion-permeable carboxysome containing intracellular carbonic anhydrase [47]. Central to the functioning of the cyanobacterial CCM is the carboxisome (Figure 4), a protein micro-compartment within the cell that contains RuBisCo and a carbonic anhydrase. The latter converts HCO_3^- into CO_2 within the carboxysome, concentrating CO_2 up to 1000-fold around the active site of RuBisCO [46], thus overcoming the inefficiency of RuBisCO [24] and its inability to distinguish O_2 from CO_2.

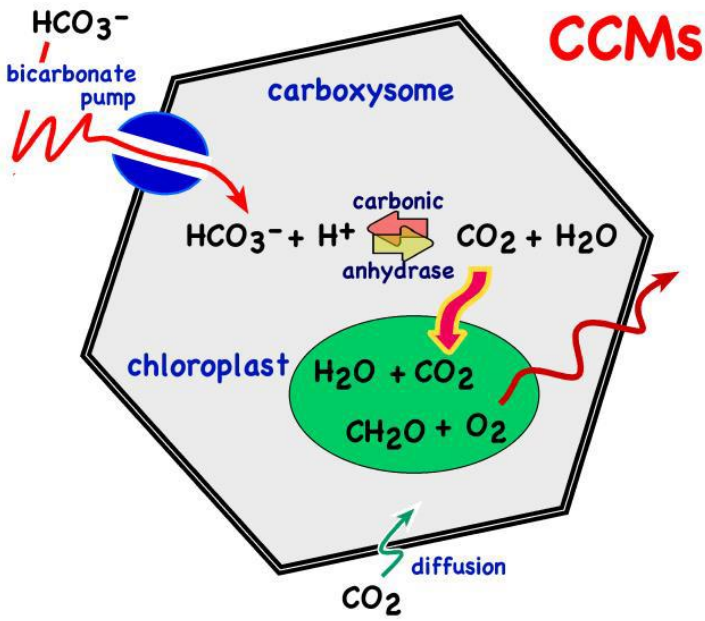

Figure 4. Central to the cyanobacterial CCM (CO_2 Concentrating Mechanism) is the carboxisome, a cellular micro-compartment containing RuBisCo and a carbonic anhydrase (CA) that, by converting HCO_3^- into CO_2, concentrates CO_2 as much as 1000-fold around the active site of RuBisCO [46]. (This figure is an original interpretation by L. Pomar based on several sources).

For eukaryotic algae with CCMs, the presence of pyrenoids is often associated with the occurrence of a CCM, although there are exceptions [47]. Eukaryotic algal CCMs likely originated independently in different clades of algae, as indicated by the diversity of inorganic C transporters and of carbonic anhydrases, as well as the lack of a strict correlation between occurrence of a CCM and the presence of a pyrenoid [47].

7. Phosphorous

Another essential element for life forms that has fluctuated downward in bioavailability through Earth history is phosphorous (P). Ranking 11th among the elements in the Earth's crust, P occurs primarily as phosphate (PO_4^{3-}) in apatite. Although found in most igneous and metamorphic rocks, mafic rocks commonly contain at least an order of magnitude more apatite than most felsic rocks (granites and rhyolites) [29]. Thus, as Fe- and Mg-rich materials have been concentrated in the Earth's mantle and core, so too has P. By the late Archean, continental-scale granitic cratons had developed on the Earth's crust, contributing to the decline in PO_4^{3-} in aquatic environments [32].

Phosphorus is one of the eleven macro-biogenic elements that make up living organisms [C, O, H, N, S, P, Na, K, Ca, Mg, Cl, Fe]. Bioavailable PO_4^{3-} is essential for all forms of life, although it has received less attention than C, N, and Fe in the evolution of autotrophy in relation to environmental changes during the last 4 Ga [48–50]. As noted in the Introduction, PO_4^{3-} is essential to cellular structure and processes, including nucleotides (DNA and RNA), phospholipid membranes, energy transfer and storage, and for synthesis of proteins and enzymes [32]. However, PO_4^{3-} became one of the most limiting nutrients for primary productivity in Phanerozoic marine ecosystems due to its low solubility in oxygenated waters and because, unlike bioavailable dissolved N (DIN), PO_4^{3-} cannot be fixed from the atmosphere [34,48,51].

Microbial uptake of PO_4^{3-} takes place through at least two kinetically distinct processes. A "low affinity component" operates continuously, apparently driven by protonmotive force. A "high affinity component" requires energy from ATP and operates when internal PO_4^{3-} pools are depleted. Was the decline in available PO_4^{3-} in Proterozoic oceans related to changes in major precipitation modes of $CaCO_3$?

A key factor in the bioavailability of PO_4^{3-} in the Archean and early Proterozoic oceans was the lack of free oxygen [42,52]. By the early Proterozoic, cyanobacteria were producing free oxygen, triggering the Great Oxidation Event (~2.4–2.1 Ga) (Figure 2). With the emergence of O_2 into the atmosphere, terrestrial weathering dramatically changed, resulting in oxidation of sulfides ubiquitous in continental rocks. A major result was the delivery of substantial amounts of sulfates to the oceans, and those dissolved sulfates provided the oxidation potential for sulphate-reducing microbes, which are obligate anaerobes. The result was an oxygenated mixed layer/photic zone to perhaps 200 m depth, but the vast ocean depths remained anoxic and sulphidic (i.e., euxinic) through most of the Proterozoic [42,52].

The bioavailability of PO_4^{3-} declined in surface waters, based on the relative insolubility of PO_4^{3-} in oxygenated waters compared to its much greater solubility in euxinic waters [51,52]. Shallow waters exposed to sunlight became depleted in PO_4^{3-} as a consequence of reduced solubility in terrestrial-runoff waters and in oxygenated surface waters, and were further diminished by biological uptake by photosynthetic cyanobacteria and microalgae, and by geochemical uptake into ferric oxyhydroxides. At the same time, the much greater volumes of subsurface, aphotic waters, which were euxinic and therefore in which PO_4^{3-} was highly soluble, became major repositories. In that respect, like today, hydrodynamic processes such as mixing and upwelling must have been critical mechanisms for supplying PO_4^{3-} to photosynthesizing microorganisms in the surface waters [51].

By the late Neoproterozoic, sufficient photosynthetic oxygen production had occurred to oxidize most oceanic waters. Two additional contributors to the increase in atmospheric O_2 and dissolved O_2 throughout the oceans were primary production by eukaryotic algae and increased solubility of O_2 in cold oceanic waters associated with Cryogenian glaciation. The latter also would have increased the rates of ocean turnover and delivery to surface waters of dissolved PO_4^{3-} from subsurface waters (Figure 5). Shen et al. [53] postulated that the oxygenation of the oceans allowed diverse animal lineages to increase in size.

On scales of major plate-tectonics processes, massive basalt flows and tectonic uplift increase delivery of weathering-mobilized PO_4^{3-} to the oceans [48,49]. On intermediate time scales, changes in rates of deep-ocean circulation influence rates of delivery of DIN and PO_4^{3-} to surface waters, where they promote primary productivity [51,54]. In some cases, regional changes in ocean circulation have brought PO_4^{3-} rich subsurface waters into oxygenated conditions, creating major phosphatization events that have resulted in economically valuable phosphate ore deposits such as the prolific Lutetian-Messinian phosphorites of Morocco [55]. Most PO_4^{3-} in the ocean is cycling within the biotic system, and is returned to seawater by microbial activity. Only a small fraction of the phosphorus is buried in sediments, as reduced conditions within the sediments promotes dissolution of PO_4^{3-} into sediment pore waters and its return to ocean cycling [54].

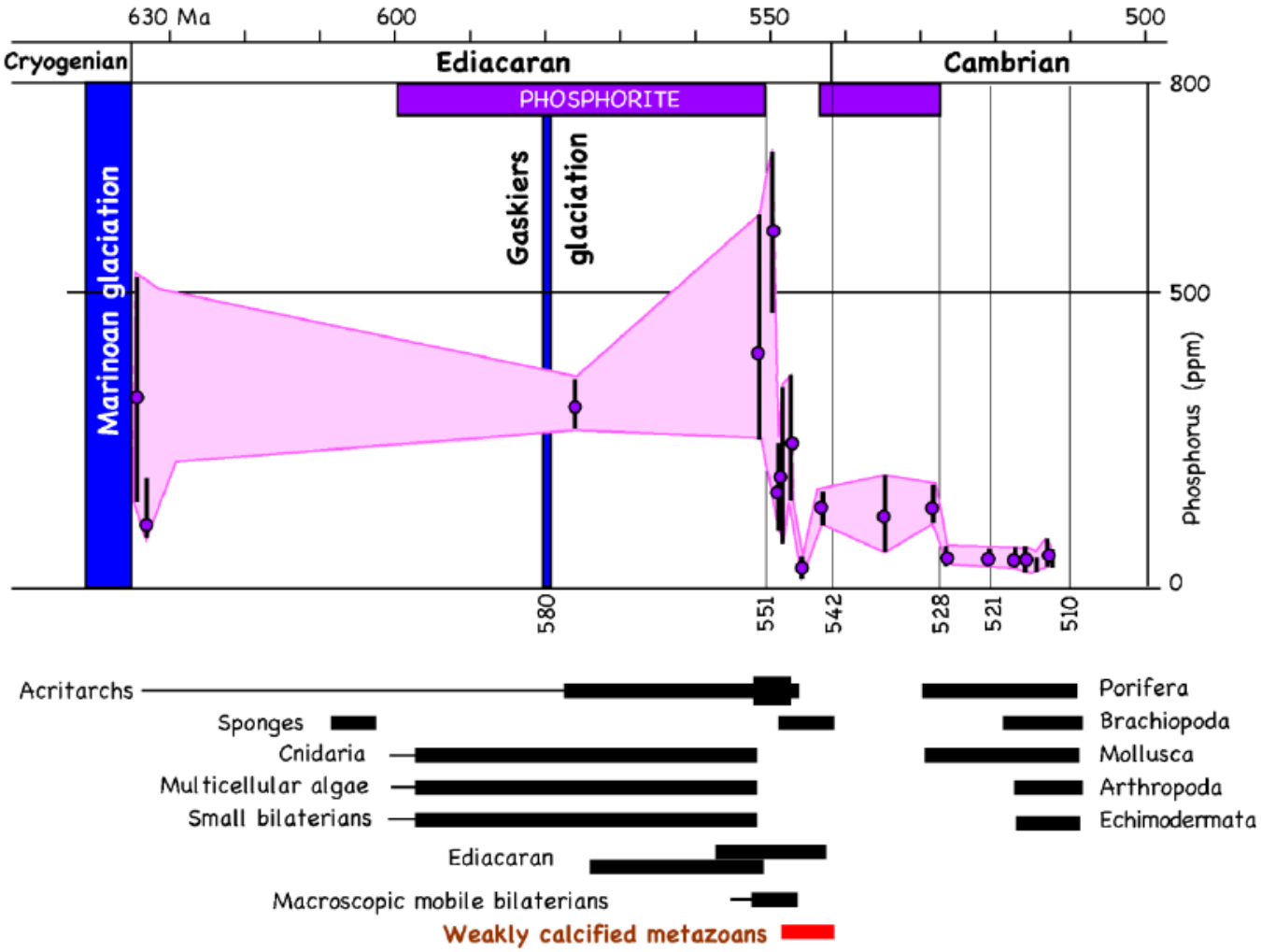

Figure 5. Evolution of Phosphorous (P) concentration through the late Neoproterozoic and Cambrian and its relationship with the emergence of major groups of organisms. Notice that the first weakly calcified metazoans (red bar) appeared during a minimum of P at the end of the Ediacaran. Modern lineages of metazoans with hard skeletons appeared by mid-Cambrian during another minimum in P concentration. (This figure is an original interpretation by L. Pomar based on numerous sources).

8. Calcification as a Sink and a Source of Both CO_2 and PO_4^{3-}

Precipitation of carbonate minerals is a long-term sink for CO_2, but in the short term, can serve as a source (e.g., [41] and references therein). Calcification typically involves two bicarbonate ions, incorporating one CO_3^{2-} into the $CaCO_3$ mineral structure and releasing the other into the environment as CO_2 [56]. In aquatic environments, photosynthetic uptake of CO_2 or HCO_3^- reduces availability of CO_2, increases pH and can lead to oversaturation with respect to calcite. Dissolved PO_4^{3-} is adsorbed onto and co-precipitates with calcite, with incorporation of some of the surface PO_4^{3-} into the bulk structure as crystal growth proceeds (Figure 6). However, higher concentrations of dissolved phosphate inhibit the growth of calcite crystals and can stop growth completely [57].

Numerous studies have documented removal of PO_4^{3-} associated with $CaCO_3$ precipitation, for example during dense blooms of some cyanobacteria. Guldbransen and Cremer [58] experimentally demonstrated co-precipitation of $CaCO_3$ and PO_4^{3-}, and Kitano et al. [59] found that stirring increases the amount of PO_4^{3-} that co-precipitates. Millero et al. [60] demonstrated that PO_4^{3-} uptake on $CaCO_3$ minerals is a multistep process. Depending upon water chemistry and temperature, adsorption or desorption can occur rapidly, in minutes to a few hours, with much slower processes lasting more

than one week. Up to 80% of the adsorbed PO_4^{3-} can be released from $CaCO_3$ over one day. The amount of PO_4^{3-} left on the $CaCO_3$ is close to equilibrium adsorption [60]. Thus, the adsorption of PO_4^{3-} during $CaCO_3$ precipitation can be both a sink and a source of phosphates (Figure 7).

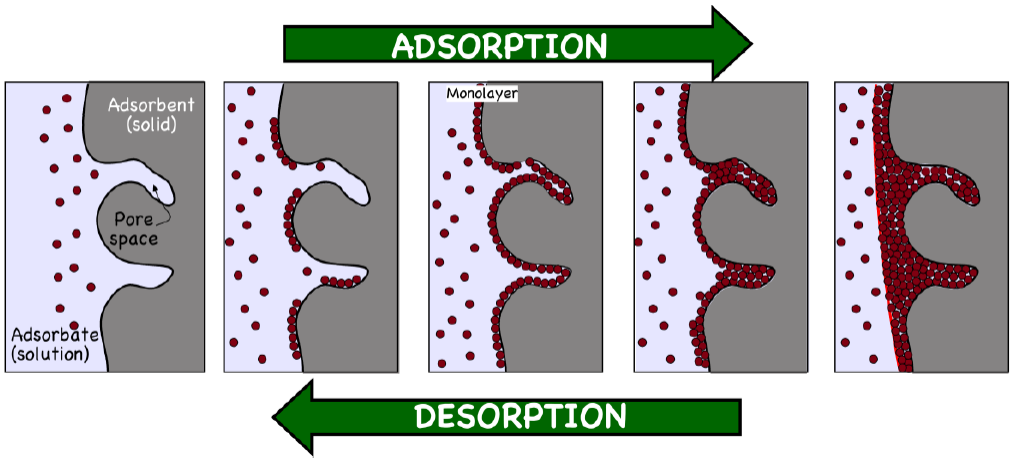

Figure 6. Simplified diagram of the adsorption process (adapted from [58–60]). Atoms, molecules or ions adhere to a surface by weak residual forces (e.g., van der Waals, electrostatic). It can be multilayer or monolayer. (This figure is an original interpretation by L. Pomar based on several sources).

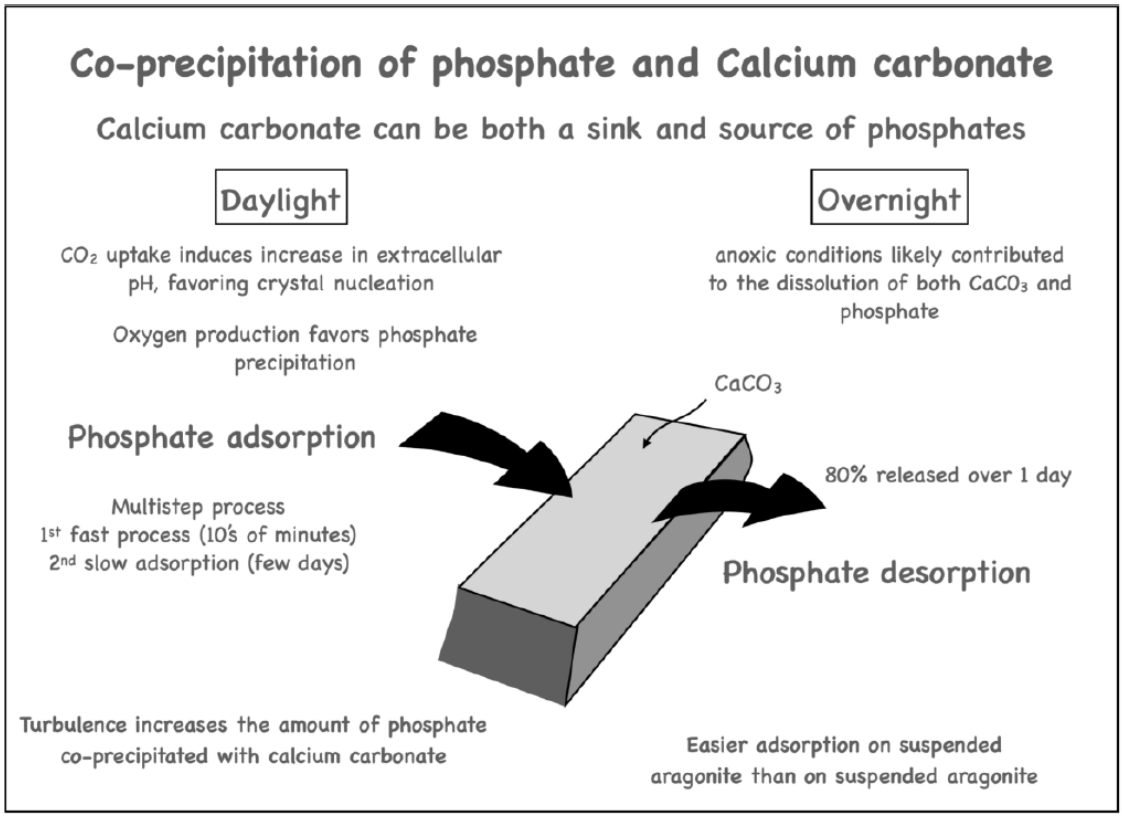

Figure 7. Co-precipitation of phosphate and calcium carbonate; note that phosphate is more readily adsorbed onto and released from aragonite than onto/from calcite ((This figure is an original interpretation by L. Pomar based on several sources, including [58–60]).

9. Prokaryotic Organo-Sedimentary Systems

Stromatolites, the fossil evidence of calcified microbial mats, can be viewed as the first biotic process to produce a hard body [61]. By the Late Archaean, ooids—the second biotic process to produce a hard body—appeared when photosynthetic O_2 production by cyanobacteria was occurring. What might have been the advantage for these benthic microbial systems to produce coated-mineral structures? Such coatings would have restricted light penetration, as well as diffusion of DIC and nutrients required for photosynthesis, growth and reproduction. Furthermore, what could be the advantage of inducing carbonate-mud precipitates (whitings) by neritic photosynthetic prokaryotes (picoplankton) and eukaryotes (phytoplankton)? This third microbially mediated organo-sedimentary system to produce carbonate precipitates emerged by the Mesoproterozoic, following the Great Oxygenation Event (GOE) (Figure 2).

Cyanobacteria have remarkably few nutritional requirements. They use light as source of energy, H_2O or H_2S as electron donors and CO_2 (or HCO_3^-) as the source of inorganic carbon [62]. Additionally, many species can fix atmospheric N_2 to NH_4^+, which makes them independent of DIN sources such as nitrate, ammonium or organic nitrogen. Hence, the most critical nutrients for cyanobacteria are PO_4^{3-}, which can be stored intracellularly as polyphosphate, and, to a lesser extent, Fe^{2+}. Both are limited by their reactivity with O_2. Moreover, cyanobacteria can minimize their PO_4^{3-} requirements through the synthesis of sulfolipids [63], allowing them to colonize low-nutrient environments, as demonstrated by their ubiquity in both terrestrial and aquatic environments.

Thus, precipitation of $CaCO_3$ during the day augments CO_2 availability for photosynthesis [64], while PO_4^{3-} adsorption sequesters that scarce but essential nutrient. At night, desorption of PO_4^{3-} makes it available for uptake by the cells. In microbial mats (Figure 8) in darkness, anoxic conditions resulting from continued sulfate reduction, aerobic respiration and sulfide oxidation likely contribute to the dissolution of $CaCO_3$ and increase the potential for PO_4^{3-} uptake by the microbial assemblage.

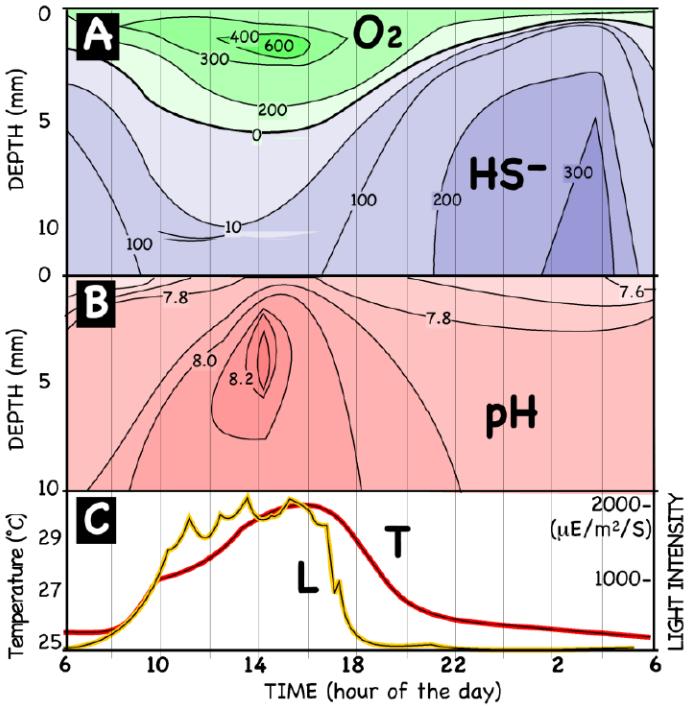

Figure 8. Oxygen and sulfide concentration (ppm) in (**A**) and pH in (**B**) variation during a diel cycle in the upper 12 mm of modern marine stromatolites in the Exuma Cays, Bahamas. (**C**): Light intensity and temperature at the surface of the stromatolite. (Adapted with permission from Ref. [65]. Copyright ©2002, American Chemical Society.).

Giant ooids, associated with cyanobacterial mats and stromatolites, are common in Late Archaean rocks. They have been described in the 2.64 Ga old Ghaap Group in South Africa [66] and in the 2.72 Ga old Pilbara group in Australia [67], becoming abundant and characteristic of many Neoproterozoic carbonates [68]. Microbially mediated organo-mineralization processes are likely involved in the origin of ooids. They can either be biologically induced (e.g., by-products of metabolic activities that increase environmental alkalinity and trigger carbonate precipitation), or biologically influenced (e.g., microbial extracellular polymeric substances can serve as templates for carbonate mineralization [69]). Again, the advantage for the microbial consortium to precipitate $CaCO_3$ coatings around particles was likely in PO_4^{3-} adsorption, associated with the precipitation of metastable amorphous carbonate [70,71] (Figure 9).

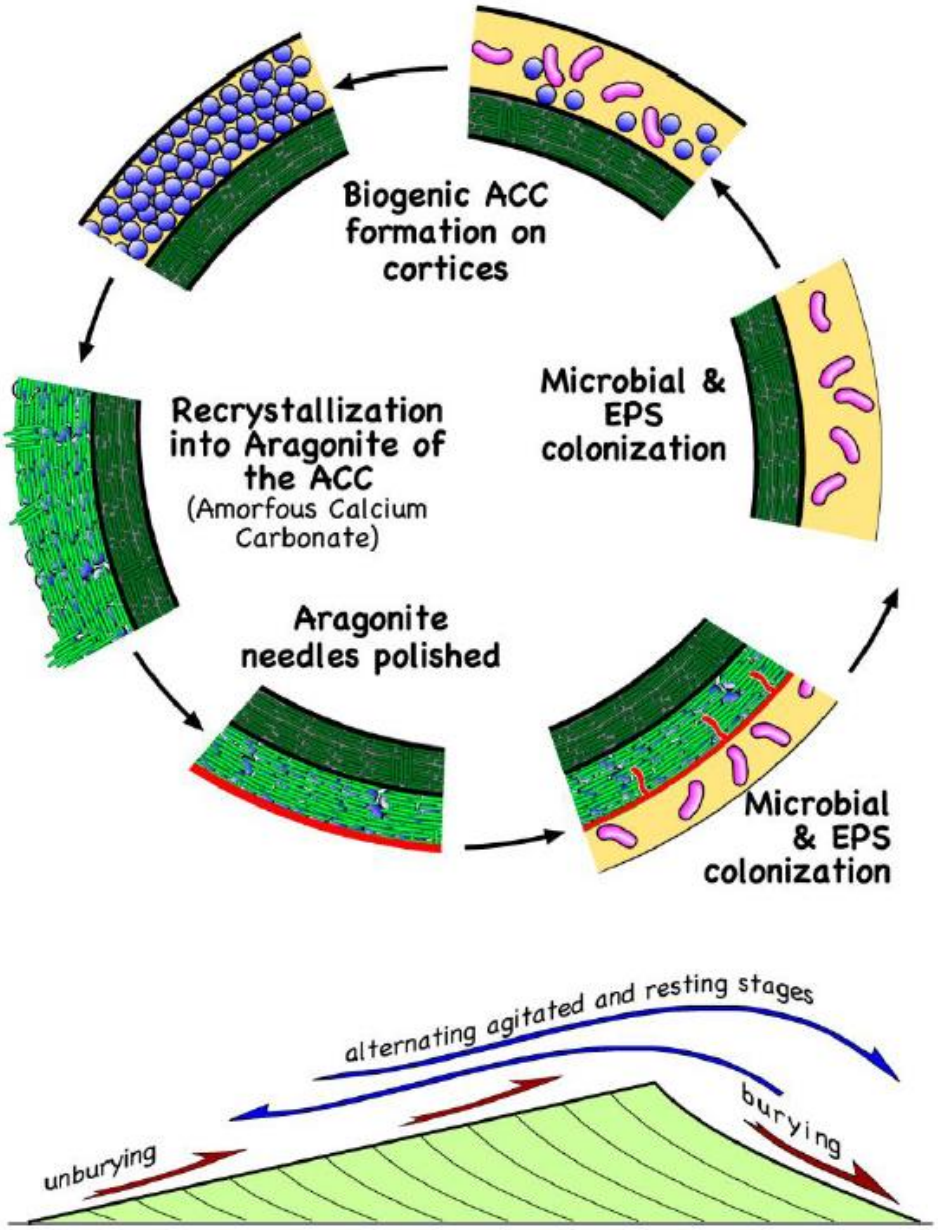

Figure 9. Conceptual multiphase model for the oolite cortex accretion. Abbreviations: ACC (amorphous $CaCO_3$) and EPS (extracellular polymeric substances). (This figure is an interpretation by L. Pomar based on cited sources [70,71]).

A significant source of lime-mud production in modern oligotrophic shallow marine and lacustrine environments also is linked to microbial calcification [72]. Whitings are the drifting milky clouds that are commonly observed in warm, shallow seas. Robbins et al. [73] estimated that whitings production might account for more than 40% of the bank-top- and peri-platform Holocene muds on the west side of Great Bahama Bank. The production of whitings is linked to blooms of cyanobacteria and planktic green algae in oligotrophic aquatic environments via CO_2 uptake [74]. Photosynthetic carbon fixation during blooms induces an increase in extracellular pH, favoring crystal nucleation [72]. What would it be the advantage for photosynthetic pico- and microplankton to induce carbonate-mud precipitation in the water? Blooming means that CO_2 and nutrient acquisition must keep pace with the increase of organic matter required for cell division. With the diurnal cycle of rapid adsorption and desorption of PO_4^{3-}, the milky cloud can efficiently capture this scarce nutrient, which would be of particular advantage in extremely oligotrophic conditions.

10. Biocalcification in Photosynthetic Eukaryotes

The basic eukaryotic cell is descended from an anaerobic Proteoarchaeota that engulfed purple, non-sulfur α-proteobacteria that could utilize oxygen but were not obligate aerobes [42,44]. All algae have that basic eukaryotic cell and all algal plastids are believed to have originated from cyanobacterial endosymbionts [42,75]. Molecular phylogenetic studies have demonstrated that the morphological diversity of the algae results from their polyphyletic origins within the Eukarya [75,76]. An interesting question then, is: Why do some marine algae within different phylogenetic groups invest energy into producing $CaCO_3$ skeletal structures, whereas most do not?

Tropical macroalgae cope with three strong selective pressures: limited access to CO_2/HCO_3^- due to warm water and competition among photosynthetic organisms, limited access to PO_4^{3-}, and herbivory. Calcification is clearly an anti-herbivory defense. Furthermore, there are striking differences in percent tissue PO_4^{3-} between calcified and fleshy algae, indicating different nutrient-acquisition strategies. The effects of nutrient enrichment with nitrogen (DIN) and PO_4^{3-} on productivity and calcification of fleshy and calcareous algae differ. DIN and PO_4^{3-} frequently enhance productivity of fleshy algae, but do not increase calcification rates of calcareous species [77].

Halimeda, a codiacean macroalga common in warm, shallow-marine environments, can add up to one segment per day, per branch (Figure 10). However, the algae require nutrient uptake for growth and reproduction in warm waters where PO_4^{3-} levels are often below detection limits. Calcification occurs during daytime within an organic matrix in the outer utricle walls of one-day-old segments. Photosynthetic removal of CO_2 by diffusion across a membrane and enzymatic anhydrase activity induces aragonite precipitation in the utricle space [78,79]. At night, respiration elevates CO_2 and decreases CO_3^{2-} saturation, which decreases seawater pH in the utricle space. The aragonite needles partially dissolve, break and recrystallize into micro-anhedral crystals (<1 μm). Such partial dissolution at night would facilitate desorption of PO_4^{3-} from the skeleton.

Coralline red algae occur as thin crusts on hard substrata that can produce free-living rhodoliths, or as thalli with articulated branches. Most precipitate high-Mg calcite rather than aragonite. Calcification dynamics (Figure 11) depend on nutrient concentrations; PO_4^{3-} inhibits the crystalline lattice and hampers calcite precipitation [80]. Enrichment of PO_4^{3-}, along with other nutrients, favors the growth of macroalgae and phytoplankton, which reduces water transparency and impedes coralline algal growth. Calcification associated with photosynthesis exhibits day-night cyclicity that is also recorded in diel pH fluctuations. Abiotic re-precipitation of $CaCO_3$ can occur in crustose-coralline red algae during nighttime [81] and pH drop at the boundary layer in darkness has been documented [82]. Thus, partial dissolution occurring at night would provide favorable conditions to remobilize adsorbed PO_4^{3-} from the calcitic skeleton and facilitate uptake by the algal cells.

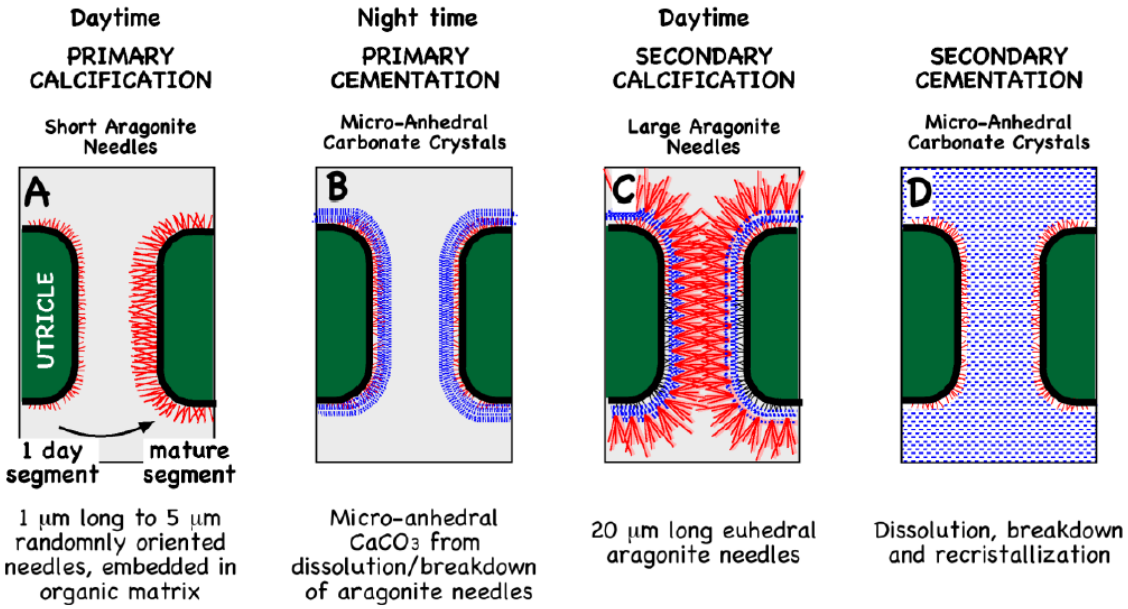

Figure 10. Calcification stages of *Halimeda* [78,79]. (**A**): Growth of short skeletal needles on the utricle wall; (**B**): recrystallization of short needles to micron-sized anhedral crystals. (**C**): secondary calcification by long, dense, euhedral, skeletal-aragonite needles, (**D**): the primary inter-utricular space in the rim of the segment is filled with micron-sized anhedral crystals. (This figure is an original interpretation by L. Pomar based on cited sources [78,79]).

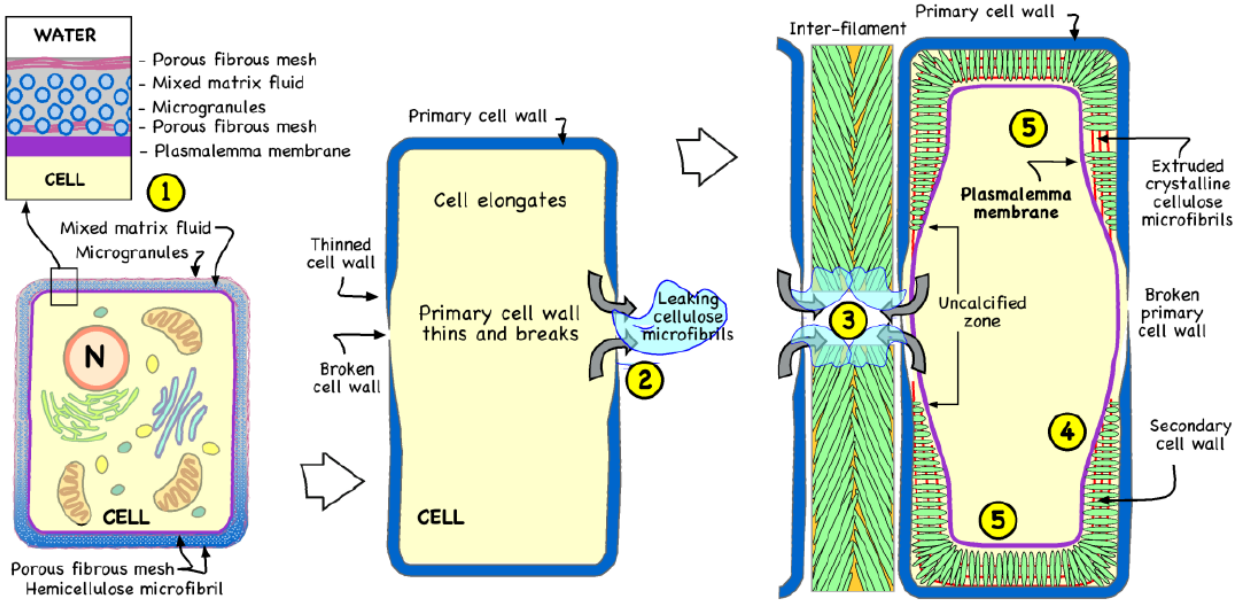

Figure 11. Skeletal formation in red algae. Process steps: (1) Primary cell wall is forming. Hemicellulose microfibrils act as nucleating substrate for micro-granules. (2) Cellulose microfibrils extrude from plasma membrane and leaks through broken primary cell wall. (3) Interfilament grains initiate attached to the external part of the primary cell wall and grow in the leaked cellulose microfibril. (4) Secondary cell wall thickens, extruded cellulose microfibrils stop leaking and mineralize as Mg-calcite. (5) Plasmalemma is pushed inward as cellulose microfibrils continue to extrude and mineralize. Secondary cell wall fully formed. (This figure is an original interpretation by L. Pomar based on sources including [80]).

Coccolithophores are photosynthetic protists that produce small calcitic disks (coccoliths). These oval-shaped plates of $CaCO_3$ consist of double discs, composed of radial

arrays of minute, elaborately-shaped crystal units. They form delicate crystalline lace or open web-like patterns in which the rate of the $CaCO_3$ crystal surface/volume is very high. Originating by the Late Triassic (Figure 2), they proliferated during the Cretaceous, and, together with planktic foraminifera, allowed widespread carbonate production in the open ocean [83]. Coccolithophores can produce as much as two coccoliths per hour [84]. The variability of coccolith shapes indicates they serve diverse functions. Young [85] noted features that defy simple physical functions, particularly complex mesh structures and the variety of elaborate forms, and suggested that coccoliths might be adaptations for nutrient uptake.

Coccolithophores thrive in waters with minimal PO_4^{3-}, that is, insufficient to promote growth of other phytoplankton. Coccolith formation is less adversely affected by nutrient deficiency than is cell division and growth [86]. The nutrient requirements for the organic cellular components of a coccolithophorid cell are similar to those for non-calcifying phytoplankton. However, forming coccoliths requires minimal nutrient cost, as coccolith production continues even when cell division ceases because of nutrient limitation [87,88].

In modern *E. huxleyi*, coccoliths nucleate and grow in a Golgi-derived coccolith vesicle, from where they migrate to the cell surface (Figure 12). Within the coccolith vesicle, polysaccharides are thought to regulate nucleation and subsequent growth of coccoliths [89]. Sviben et al. [90] identified a reservoir compartment, distinct from the coccolith vesicle, with high concentrations of Ca^{2+} and PO_4^{3-}. Only Ca^{2+} is delivered to the coccolith vesicle [91], whereas PO_4^{3-} is diverted to the cell for growth and reproduction.

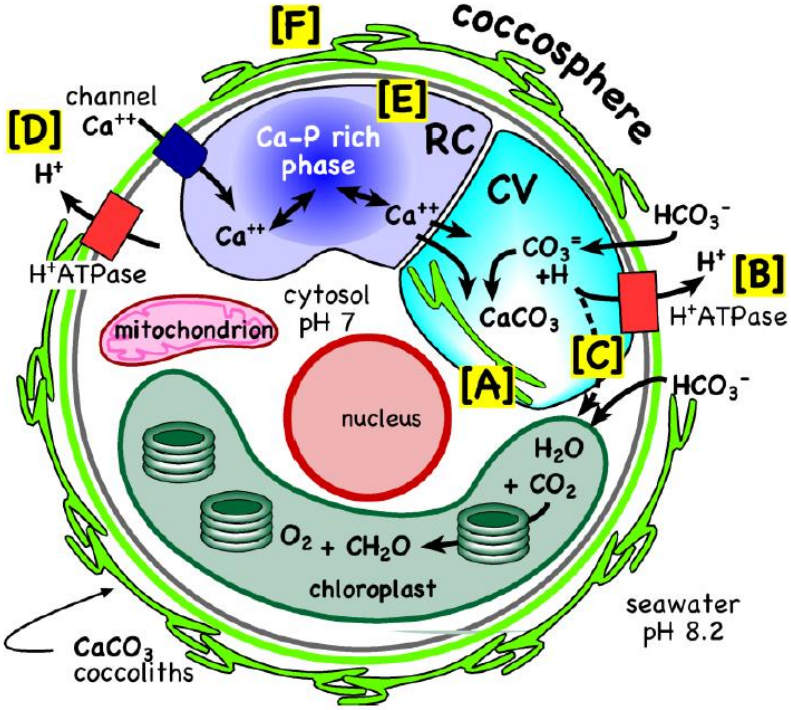

Figure 12. Calcification processes in coccolithophorids. [**A**] Coccolith formation occurs within the Golgi-derived coccolith vacuole (CV). [**B**] Intracellular $CaCO_3$ precipitation from bicarbonate (HCO_3^-) releases equimolar H^+ that must be rapidly removed from the CV to maintain pH for $CaCO_3$ precipitation. [**C**] Some H^+ may be utilized by photosynthesis. [**D**] Though not fully understood, it is hypothesized that Ca^{2+} is recruited through Ca-channels and V-type ATPase pumps. [**E**] A reservoir compartment (RC) concentrates Ca^{++} and PO_4^{3-}. [**F**] The coccolith-associated polysaccharide may drive the Ca^{2+} from the coccosphere into the RC, from where only Ca^{2+} is transported to the coccolith vesicle (CV) and PO_4^{3-} is diverted to the cell for algal growth and reproduction. Transfer of Ca^{2+} from the RC into the CV uses Ca^{2+} channels and transporters. (This figure is an original interpretation by L. Pomar based on [88–91] and other sources).

11. CO_2 and Carbonate Depositional History

In aqueous solutions, CO_3^{2-}, HCO_3^-, CO_2, and H_2CO_3 co-exist in dynamic equilibria (Figure 3). When CO_2 reacts with water (H_2O), it complexes to H_2CO_3, which dissociates to H^+ and HCO_3^-, thereby increasing the concentration of H^+ and cause the seawater acidity to increase (i.e., the pH to decline). When $CaCO_3$ (e.g., limestone) reacts with free hydrogen (H^+) ions in seawater, the solid $CaCO_3$ dissolves, forming free calcium (Ca^{++}) ions and free bicarbonate (HCO_3^-) ions. As noted previously, the concentrations of ions of carbonate, bicarbonate, phosphate, borate, orthosilicate, sulfides, and organic acids constitute alkalinity in aquatic environments, especially HCO_3^-. The consumption of protons results in decreased H^+ activity. Thus, $CaCO_3$ acts to neutralize or buffer the solution by consuming H^+.

In the modern world, burning of fossil fuels, combined with widespread changes in land use, have resulted in rapidly increasing concentrations of atmospheric CO_2 that are causing the decline in the pH of surface seawater (e.g., [6–11]). Will the progressive warming and acidification cause mass extinctions and evolutionary turnover of marine biotas, as has been documented by paleoclimatic evidence [15–17]?

From this question emerges another major "carbonate paradox". Contrary to predictions of increased carbonate dissolution in response to increasing CO_2, extended high CO_2 Greenhouse World periods during the Phanerozoic (Silurian–Devonian and Jurassic–Cretaceous) were characterized by thick and extensive accumulations of fine-grained carbonates associated with cyanobacterial and algal calcification, commonly baffled by skeletal carbonates (e.g., stromatoporids, corals, rudists) (Figure 2) ([92] and references therein). In the Cenozoic, coral reefs emerged as major carbonate factories as Icehouse World conditions developed and became predominant in the Oligocene through the Holocene, a conundrum noted by Frost many years ago [31].

The solution to this paradox lies in two parts. First, there is the "rate" factor. Mass extincton events in the Phanerozoic record have long be recognized by carbonate depositional hiatuses that indicate times of global carbonate dissolution [93]. Very rapid increases in atmospheric CO_2 (Figure 3) or other atmospheric compounds that unite with water to form acids (e.g., $2SO_2 + H_2O \rightarrow H_2SO_4 + 2H^+$), whether caused by massive extrusion of flood basalts, bolide impact, methane-hydrate release, extensive burning of fossil fuels, or some combination of events, can indeed trigger carbonate dissolution resulting in hiatuses of tens of thousands of years (Paleocene–Eocene) or hundreds of thousand years (Cretaceous–Paleocene) [94] and references therein) or millions of years (Permian–Triassic) [17].

However, eventually terrestrial weathering and dissolution under high atmospheric CO_2 over time increased alkalinity and restored the carbonate factory. The massive accumulations of Silurian–Devonian and Jurassic–Cretaceous carbonates occurred during times of relatively rapid sea-floor spreading, which elevated both CO_2 and Ca^{2+} concentrations, triggered warming temperatures, sea-level rise, and expansive areas of relatively shallow basins and shelves. Reduced land areas limited freshwater input of dissolved nutrients and warm waters reduced rates of deep-ocean circulation. During Greenhouse-world conditions, the trophic resource continuum expanded (compared to Icehouse conditions), with limited extremely rich regions of upwelling and expansive regions of extreme oligotrophy, the latter fostering extensive production of carbonates [95]. Elevated evaporation rates, relatively shallow seas, and high alkalinity favored calcifying cyanobacterial and algal taxa that could sequester scarce PO_4^{3-} while producing excess organic matter upon which calcifying animals (e.g., rudists) could also thrive [92]. The name Cretaceous was actually derived from the Latin *creta*, meaning chalk [96].

During daylight hours, in warm, shallow waters, abundant microalgae take up available DIN and PO_4^{3-}, while high rates of photosynthesis deplete immediate access to CO_2/HCO_3^-. Calcification associated with photosynthesis alleviates both deficiencies. Two HCO_3^- provides one CO_2 for photosynthesis and a CO_3^{2-} for calcification, somewhat alleviating local CO_2 depletion. At the same time, PO_4^{3-} adsorption occurs during daytime calcification and is partially desorbed at night, becoming available for uptake by the

cyanobacteria or algae. In addition, some dissolution of the $CaCO_3$ releases HCO_3^-, and along with community respiration, results in early morning maximum concentrations of HCO_3^-. With the onset of light, photosynthesis makes energy available to CCMs, providing the primary producers with access to and storage of CO_2, which becomes increasingly unavailable over the course of the day.

Finally, why did extensive coral reefs only become prevalent with the onset of the Icehouse World climates [31]? Again, the answer is likely climatic and geochemical influences on biological processes [92,97–100]. High-latitude cooling, compression of tropical habitats, and increasing temperature gradients between high and low latitudes and between surface and deeper waters [97] were major factors. Coral communities flourished circumtropically beginning in the late Oligocene [31]. By the early Miocene, reefs and associated biota expanded latitudinal distributions by more than 10° north and south [98]. The expansion in reef-building capacity corresponded to increasing Mg/Ca ratios in seawater [99] and falling atmospheric CO_2 concentrations [100], both of which promoted aragonite precipitation in warm, tropical waters. The majority of extant Symbiodiniacea lineages diversified since Middle Miocene [101]. Global cooling, including much cooler subsurface waters, likely benefited the coral-Symbiodiniacea symbioses, which are sensitive to photo-oxidative stress under elevated temperatures [102]. The substantial increase in rates of circulation of deep, cold waters resulted in more "intermediate" conditions of oceanic oligotrophy [95]. Pomar and Hallock [92] further postulated that Neogene cooling supported the co-evolution and expansion of zooxanthellate corals and coralline algae into shallow, high-energy waters, where their carbonate production potential was highest. In such environments, both calcification and PO_4^{3-} extraction are also potentially optimized.

12. Conclusions

Photosynthesis typically involves daytime CO_2 uptake and O_2 release predominating over respiration; at night, respiration consumes O_2 and releases CO_2. The result is strong diel variation in both pH and dissolved O_2 concentrations in aquatic environments. In warm-water environments in which alkalinity is relatively high and PO_4^{3-} concentrations are minimal, these variations have the potential to promote precipitation of $CaCO_3$ and associated adsorption of PO_4^{3-} in daylight when photosynthesis is active. At night, lower pH and oxygen availability can promote some $CaCO_3$ dissolution and PO_4^{3-} desorption. The combination of calcification and PO_4^{3-} extraction occurs in photosynthesizing cyanobacteria, as well as in a diverse array of calcifying nanophytoplankton and calcareous macroalgae, indicating that this process allows both prokaryotic and eukaryotic photosynthetic organisms to thrive in warm, alkaline, oligotrophic waters. Concentrations of both atmospheric CO_2 and surface-ocean PO_4^{3-}, which are essential for biological productivity, have declined by at least 1–2 orders of magnitude over Earth history. **The Phosphate Extraction Mechanism**, associated with photosynthetically induced calcification, has played a major role in the production and accumulation of carbonates throughout much of the Proterozoic and the Phanerozoic. Recognition of this relationship helps resolve the apparent paradox that periods in the Phanerozoic when atmospheric CO_2 levels were considerably higher than present (as well as higher than predicted Anthropocene concentrations) were times of massive accumulation of carbonates, predominantly produced by photosynthesizing cyanobacteria and calcifying algae. This synthesis also stresses the importance of rates of change, as times of rapid increase in atmospheric CO_2 concentrations were associated with mass-extinction events characterized by global carbonate-depositional hiatuses, requiring hundreds of thousands or even millions of years for surface waters of the oceans to regain sufficient alkalinity to sustain accumulation of massive carbonates.

Author Contributions: Conceptualization: L.P., P.H., G.M.-V. and J.I.B.; Methodology: L.P., P.H., G.M.-V. and J.I.B.; Investigation: L.P., P.H., G.M.-V. and J.I.B.; Writing: Original Draft Preparation, L.P. and P.H.; Writing: Review and Editing, P.H. and G.M.-V. All authors have read and agreed to the published version of the manuscript.

Funding: JIB acknowledges funding from the Basque Government to the Research Group IT1602-22. L.P., P.H. and G.M.-V. participation did not involved external funding aside from their academic institutions.

Institutional Review Board Statement: Not applicable.

Informed Consent Statement: Not applicable.

Data Availability Statement: Not applicable.

Acknowledgments: Gabriel Moyà (UIB) for the seminal discussions on this topic, and to the volume editor, H. Westphal, for her patience and suggestions.

Conflicts of Interest: The authors declare no conflict of interest.

References

1. Selly, R.C.; Sonnenberg, S.A. *Elements of Petroleum Geology*, 3rd ed.; Academic Press: Boston, USA, 2015; pp. 1–507.
2. Kharecha, P.; Kasting, J.; Siefert, J. A coupled atmosphere–ecosystem model of the early Archean Earth. *Geobiology* **2005**, *3*, 53–76. [CrossRef]
3. Morse, J.W.; Arvidson, R.S.; Lüttge, A. Calcium carbonate formation and dissolution. *Chem. Rev.* **2007**, *107*, 342–381. [CrossRef] [PubMed]
4. Burton, M.R.; Sawyer, G.M.; Granieri, D. Deep carbon emissions from volcanoes. *Rev. Mineral. Geochem.* **2013**, *75*, 323–354. [CrossRef]
5. Global Carbon Budget 2021. *Earth Syst. Sci. Data* **2022**, *14*, 1917–2005. [CrossRef]
6. Keeling, C.D. The concentration and isotopic abundances of carbon dioxide in the atmosphere. *Tellus* **1960**, *12*, 200–203. [CrossRef]
7. Scripps CO2 Program. Global Stations CO2 Concentration Trends. 2022. Available online: https://scrippsco2.ucsd.edu/graphics_gallery/other_stations/global_stations_CO2_concentration_trends.html (accessed on 19 September 2022).
8. Harris, D.C. Charles David Keeling and the story of atmospheric CO_2 measurements. *Anal. Chem.* **2010**, *82*, 7865–7870. [CrossRef]
9. IPCC (Intergovernment Panel on Climate Change). Available online: https://www.ipcc.ch/about/ (accessed on 22 August 2022).
10. Kleypas, J.A.; Buddemeier, R.W.; Archer, D.; Gattuso, J.-P.; Langdon, C.; Opdyke, B.N. Geochemical consequences of increased atmospheric CO_2 on coral reefs. *Science* **1999**, *284*, 118–120. [CrossRef]
11. Caldeira, K.; Wickett, M.E. Anthropogenic carbon and ocean pH. *Nature* **2003**, *425*, 365. [CrossRef]
12. Wigley, T.M. A combined mitigation/geoengineering approach to climate stabilization. *Science* **2006**, *314*, 452–454. [CrossRef]
13. Wolf-Gladrow, D.; Riebesell, U.; Burkhardt, S.; Bijma, J. Direct effects of CO_2 concentration on growth and isotopic composition of marine plankton. *Tellus* **1999**, *51B*, 461–476. [CrossRef]
14. Orr, J.C.; Fabry, V.J.; Aumont, O.; Bopp, L.; Doney, S.C.; Feely, R.A.; Gnanadesikan, A.; Gruber, N.; Ishida, A.; Joos, F.; et al. Anthropogenic ocean acidification over the twenty-first century and its impact on calcifying organisms. *Nature* **2005**, *437*, 681–686. [CrossRef] [PubMed]
15. Veron, J.E.N. Mass extinctions and ocean acidification: Biological constraints on geological dilemmas. *Coral Reefs* **2008**, *27*, 459–472. [CrossRef]
16. Kiessling, W.; Simpson, C. On the potential for ocean acidification to be a general cause of ancient reef crises. *Glob. Chang. Biol.* **2011**, *17*, 56–67. [CrossRef]
17. Clarkson, M.O.; Kasemann, S.A.; Wood, R.A.; Lenton, T.M.; Dains, S.J.; Richoz, S.; Ohnemüller, F.; Meixner, A.; Poulton, S.W.; Tipper, E. Ocean acidification and the Permo-Triassic Mass Extinction. *Science* **2015**, *348*, 229–232. [CrossRef] [PubMed]
18. Dodd, M.; Papineau, D.; Grenne, T.; Slack, J.F.; Rittner, M.; Pirajno, F.; O'Neil, J.; Little CT, S. Evidence for early life in Earth's oldest hydrothermal vent precipitates. *Nature* **2017**, *543*, 60–64. [CrossRef]
19. Nutman, A.P.; Bennett, V.C.; Friend CR, L.; Van Kranendonk, M.J.; Chivas, A.R. Rapid emergence of life shown by discovery of 3700-million-year-old microbial structures. *Nature* **2016**, *537*, 535–538. [CrossRef]
20. Krissansen-Totton, J.; Arney, G.N.; Catling, D.C. Constraining the climate and ocean pH of the early Earth with a geological carbon cycle model. *Proc. Natl. Acad. Sci. USA* **2018**, *115*, 4105–4110. [CrossRef]
21. Holland, H.D. The oxygenation of the atmosphere and oceans. *Phil. Trans. R. Soc. B-Biol. Sci.* **2006**, *362*, 903–915. [CrossRef]
22. Kasting, J.F. Earth's early atmosphere. *Science* **1993**, *259*, 920–926. [CrossRef]
23. Kaufman, A.J.; Xiao, S. High CO_2 levels in the Proterozoic atmosphere estimated from analyses of individual microfossils. *Nature* **2003**, *425*, 279–282. [CrossRef]
24. Kah, L.C.; Bartley, J.K. Effect of marine carbon reservoir size on the duration of carbon isotope excursions. Interpreting the Mesoproterozoic carbon isotope record. *Geol. Soc. Am. Abstr. Programs* **2004**, *36*, 78.
25. Berner, R.A.; Kothavala, Z. GEOCARB III: A revised model of atmospheric CO_2 over Phanerozoic time. *Am. J. Sci.* **2001**, *301*, 182–204. [CrossRef]
26. Royer, D.L.; Berner, R.A.; Montañez, I.P.; Tabor, N.J.; Beerling, D.J. CO_2 as a primary driver of Phanerozoic climate. *GSA Today* **2014**, *14*, 4–10. [CrossRef]
27. Kah, L.C.; Riding, R. Mesoproterozoic carbon dioxide levels inferred from calcified cyanobacteria. *Geology* **2007**, *35*, 799–802. [CrossRef]

28. Sheldon, N.D. Precambrian paleosols and atmospheric CO_2 levels. *Precambrian Res.* **2006**, *147*, 148–155. [CrossRef]
29. Sleep, N.H.; Zahnle, K. Carbon dioxide cycling and implications for climate on ancient Earth. *J. Geophys. Res.* **2001**, *106*, 1373–1399. [CrossRef]
30. Riding, R. Cyanobacterial calcification, carbon dioxide concentrating mechanisms, and Proterozoic–Cambrian changes in atmospheric composition. *Geobiology* **2006**, *4*, 299–316. [CrossRef]
31. Frost, S.H. Cenozoic reef systems of Caribbean. Prospects for paleoecologic synthesis. *Am. Assoc. Petrol. Geol. Stud. Geol.* **1977**, *4*, 93–110.
32. Kempe, S.; Degens, E.T. An early soda ocean. *Chem. Geol.* **1985**, *53*, 95–108. [CrossRef]
33. Crockford, P.; Halevy, I. Questioning the paradigm of a phosphate-limited Archaean biosphere. *Geophys. Res. Let.* **2022**, *49*, e2022GL099818. [CrossRef]
34. Ingalls, M.; Grotzinger, J.P.; Present, T.; Rasmussen, B.; Fischer, W.W. Carbonate-associated phosphate (CAP) indicates elevated phosphate availability in Neoarchean shallow marine environments. *Geophys. Res. Let.* **2022**, *49*, e2022GL098100. [CrossRef]
35. Zahnle, K.; Arndt, N.; Cockell, C.; Halliday, A.; Nisbet, E.; Selsis, F.; Sleep, N.H. Emergence of a habitable planet. *Space Sci. Rev.* **2007**, *129*, 35–78. [CrossRef]
36. Sleep, N.H. The Hadean-Archaean environment. *Cold Spring Harb. Perspect. Biol.* **2010**, *2*, a002527. [CrossRef] [PubMed]
37. O'Neil, J.; Carlson, R.W.; Francis, D.; Stevenson, R.K. Neodymium-142 evidence for Hadean mafic crust. *Science* **2009**, *321*, 1828–1831. [CrossRef]
38. Sleep, N.H.; Zahnle, K.; Neuhoff, P.S. Initiation of clement surface conditions on the early Earth. *Proc. Natl. Acad. Sci. USA* **2001**, *98*, 3666–3672. [CrossRef]
39. Lowe, D.R. Abiological origin of described stromatolites older than 3.2 Ga. *Geology* **1994**, *22*, 387–390. [CrossRef]
40. Goldblatt, C.; Zahnle, K.J. Clouds and the faint young Sun paradox. *Clim. Past* **2011**, *7*, 203–220. [CrossRef]
41. Hallock, P. Changing influences between life and limestones in Earth history. In *Coral Reefs in the Anthropocene*; Birkeland, C., Ed.; Springer: Dordrecht, The Netherlands, 2015; pp. 17–42.
42. Mentel, M.; Martin, W. Energy metabolism among eukaryotic anaerobes in light of Proterozoic ocean chemistry. *Phil. Trans. R. Soc. B-Biol. Sci.* **2008**, *363*, 2717–2729. [CrossRef]
43. Ward, L.M.; Rasmussen, B.; Fischer, W.W. Primary productivity was limited by electron donors prior to the advent of oxygenic photosynthesis. *J. Geophys. Res. Biogeosci.* **2019**, *124*, 211–226. [CrossRef]
44. Fischer, W.W.; Hemp, J.; Johnson, J.E. Evolution of oxygenic photosynthesis. *Ann. Rev. Earth Planet. Sci.* **2016**, *44*, 647–683. [CrossRef]
45. Erb, T.J.; Zarzycki, J. A short history of RubisCO: The rise and fall (?) of Nature's predominant CO_2 fixing enzyme. *Curr. Opin. Biotech.* **2018**, *49*, 100–107. [CrossRef] [PubMed]
46. Badger, M.R.; Price, G.D. CO_2 concentrating mechanisms in cyanobacteria: Molecular components, their diversity and evolution. *J. Exper. Bot.* **2003**, *54*, 609–622. [CrossRef] [PubMed]
47. Raven, J.A.; Beardall, J.; Sánchez-Baracaldo, P. The possible evolution and future of CO_2-concentrating mechanisms. *J. Exper. Bot.* **2017**, *68*, 3701–3716. [CrossRef] [PubMed]
48. Papineau, D. Global biogeochemical changes at both ends of the Proterozoic: Insights from phosphorites. *Astrobiology* **2010**, *10*, 165–181. [CrossRef]
49. Large, R.R.; Halpin, J.A.; Lounejeva, E.; Danyushevsky, L.V.; Maslennikov, V.V.; Gregory, D.; Sack, P.J.; Haines, P.W.; Long, J.A.; Makoundi, C.; et al. Cycles of nutrient trace elements in the Phanerozoic ocean. *Gondwana Res.* **2015**, *28*, 1282–1293. [CrossRef]
50. Pufahl, P.K.; Groat, L.A. Sedimentary and igneous phosphate deposits: Formation and exploration: An invited paper. *Econ. Geol.* **2017**, *112*, 483–516. [CrossRef]
51. Paytan, A.; McLaughlin, K. The oceanic phosphorus cycle. *Chem. Rev.* **2007**, *107*, 563–576. [CrossRef]
52. Poulton, S.W.; Canfield, D.E. Ferruginous conditions: A dominant feature of the ocean through Earth's history. *Elements* **2011**, *7*, 107–112. [CrossRef]
53. Shen, J.; Webb, G.A.; Jell, J.S. Platform margins, reef facies and microbial carbonates; a comparison of Devonian reef complexes in the Canning Basin, Western Australia and the Guilin region, South China. *Earth-Sci. Rev.* **2008**, *88*, 33–59. [CrossRef]
54. Baturin, G.N. Phosphorus cycle in the ocean. *Lithol. Min. Res.* **2003**, *38*, 101–119. [CrossRef]
55. Chernoff, C.B.; Orris, G.J. Data set of world phosphate mines, deposits, and occurrences: Part A. geologic data; Part B. location and mineral economic data. *U.S. Geol. Surv. Open-File Rep.* **2002**, *C6*, 680.
56. Vescei, A.; Berger, W.H. Increase of atmospheric CO_2 during deglaciation: Constraints on the coral reef hypothesis from patterns of deposition. *Glob. Biogeochem. Cycles* **2004**, *18*, GB1035.
57. Danen-Louwerse, H.J.; Lijklema, L.; Coenraats, M. Coprecipitation of phosphate with calcium carbonate in Lake Veluwe. *Water Resour.* **1995**, *29*, 1781–1785. [CrossRef]
58. Gulbrandsen, R.A.; Cremer, M. Coprecipitation of carbonate and phosphate from seawater. *U.S. Geol. Surv. Prof. Pap.* **1970**, *700-C*, C125–C126.
59. Kitano, Y.; Okumura, M.; Idogaki, M. Uptake of phosphate ions by calcium carbonate. *Geochem. J.* **1978**, *12*, 29–37. [CrossRef]
60. Millero, F.; Huang, F.; Zhu, X.; Liu, X.; Zhang, J.-Z. Adsorption and desorption of phosphate on calcite and aragonite in seawater. *Aquat. Geochem.* **2001**, *7*, 33–56. [CrossRef]

61. Dupraz, C.; Reid, R.P.; Braissant, O.; Decho, A.W.; Norman, R.S.; Visscher, P.T. Processes of carbonate precipitation in modern microbial mats. *Earth-Sci. Rev.* **2009**, *96*, 141–162. [CrossRef]
62. Stal, L.J. Coastal microbial mats: The physiology of a small-scale ecosystem. *S. Afr. J. Bot.* **2001**, *67*, 399–410. [CrossRef]
63. Van Mooy, B.A.S.; Rocap, G.; Fredricks, H.F.; Evans, C.T.; Devol, A.H. Sulfolipids dramatically decrease phosphorus demand by picocyanobacteria in oligotrophic marine environments. *Proc. Natl. Acad. Sci. USA* **2006**, *103*, 8607–8612. [CrossRef]
64. McConnaughey, T.A.; Whelan, J.F. Calcification generates protons for nutrient and bicarbonate uptake. *Earth-Sci. Rev.* **2006**, *42*, 95–117. [CrossRef]
65. Visscher, P.T.; Hoeft, S.E.; Surgeon, T.-M.L.; Rogers, D.R.; Bebout, B.M.; Thompson, J.S.; Reid, R.P. Microelectrode measurements in stromatolites. Unraveling the Earth's past? In *Environmental Electrochemistry: Analyses of Trace Element Biogeochemistry*; ACS Symposium Series 811; Taillefert, M., Rozan, T., Eds.; Oxford University Press: New York, NY, 2002; pp. 265–282.
66. Wright, D.T.; Altermann, W. Microfacies development in Late Archaean stromatolites and oolites of the Ghaap Group of South Africa. *Geol. Soc. Lond. Spec. Pub.* **2000**, *178*, 51–70. [CrossRef]
67. Batchelor, M.T.; Burne, R.V.; Henry, B.I.; Li, F.; Paul, P. A biofilm and organomineralisation model for the growth and limiting size of ooids. *Sci. Rep.* **2018**, *8*, 559. [CrossRef] [PubMed]
68. Grotzinger, J.P.; James, N.P. Precambrian carbonates: Evolution of understanding. In *Carbonate Sedimentation and Diagenesis in the Evolving Precambrian World*; Grotzinger, J.P., James, N.P., Eds.; SEPM Society for Sedimentary Geology Special Publications: Tulsa, OK, USA, 2000; Volume 67, pp. 3–20.
69. Brehm, U.; Krumbein, W.E.; Palinska, K.A. Biomicrospheres generate ooids in the laboratory. *Geomicrobiol. J.* **2006**, *23*, 545–550. [CrossRef]
70. Diaz, M.R.; Eberli, G.P.; Blackwelder, P.; Phillips, B.; Swart, P.K. Microbially mediated organomineralization in the formation of ooids. *Geology* **2017**, *45*, 771–774. [CrossRef]
71. Diaz, M.R.; Eberli, G.P. Decoding the mechanism of formation in marine ooids: A review. *Earth-Sci. Rev.* **2019**, *190*, 536–556. [CrossRef]
72. Yates, K.K.; Robbins, L.L. Microbial lime-mud production and its relation to climate change. In *Geological Perspectives of Global Climate Change*; Gerhard, L.C., Harrison, W.H., Hanson, B.M., Eds.; American Association of Petroleum Geologists: Tulsa, OK, USA, 2001; Volume 47, pp. 267–283.
73. Robbins, L.L.; Tao, Y.; Evans, C.A. Temporal and spatial distribution of whitings on Great Bahama Bank and a new lime mud budget. *Geology* **1997**, *25*, 947–950. [CrossRef]
74. Robbins, L.L.; Blackwelder, P.L. Biochemical and ultrastructural evidence for the origin of whitings: A biologically induced calcium carbonate precipitation mechanism. *Geology* **1992**, *20*, 464–468. [CrossRef]
75. Bhattacharya, D.; Medlin, L. The phylogeny of plastids: A review based on comparisons of small-subunit ribosomal RNA coding regions. *J. Phycol.* **1995**, *31*, 489–498. [CrossRef]
76. Stiller, J.W.; Hall, B.D. The origin of the red algae: Implications for plastid evolution. *P. Natl. Acad. Sci. USA* **1997**, *94*, 4520–4525. [CrossRef]
77. Demes, K.W.; Littler, M.M.; Littler, D.S. Comparative phosphate acquisition in giant-celled rhizophytic algae (Bryopsidales, Chlorophyta): Fleshy vs. calcified forms. *Aquat. Bot.* **2010**, *92*, 157–160. [CrossRef]
78. Wizemann, A.; Meyer, F.W.; Westphal, H. A new model for the calcification of the green macro-alga *Halimeda opuntia* (*Lamouroux*). *Coral Reefs* **2015**, *33*, 951–964. [CrossRef]
79. Wizemann, A.; Meyer, F.W.; Hofmann, L.C.; Wild, C.; Westphal, H. Ocean acidification alters the calcareous microstructure of the green macro-alga *Halimeda opuntia*. *Coral Reefs* **2015**, *34*, 941–954. [CrossRef]
80. Nash, M.C.; Diaz-Pulido, G.; Harvey, A.S.; Adey, W. Coralline algal calcification: A morphological and process-based understanding. *PLoS ONE* **2019**, *14*, e0221396. [CrossRef] [PubMed]
81. Comeau, S.; Edmunds, P.J.; Spindel, N.B.; Carpenter, R.C. The responses of eight coral reef calcifiers to increasing partial pressure of CO_2 do not exhibit a tipping point. *Limnol. Oceanogr.* **2003**, *58*, 388–398. [CrossRef]
82. Hurd, C.L.; Cornwall, C.E.; Currie, K.; Hepburn, C.D.; McGraw, C.M.; Hunter, K.A.; Boyd, P.W. Metabolically induced pH fluctuations by some coastal calcifiers exceed projected 22nd century ocean acidification: A mechanism for differential susceptibility? *Glob. Chang. Biol.* **2011**, *17*, 3254–3262. [CrossRef]
83. Hay, W.W. Carbonate fluxes and calcareous nannoplankton. In *Coccolithophores–From Molecular Processes to Global Impact*; Thierstein, H., Young, J.R., Eds.; Springer: New York, NY, USA, 2004; pp. 509–527.
84. Monteiro, F.M.; Bach, L.T.; Brownlee, C.; Bown, P.; Rickaby RE, M.; Poulton, A.J.; Tyrrell, T.; Beaufort, L.; Dutkiewicz, S.; Gibbs, S.; et al. Why marine phytoplankton calcify. *Sci. Adv.* **2016**, *2*, e1501822. [CrossRef]
85. Young, J.R. Possible functional interpretations of coccolith morphology. *Abh. Geolog. Bundesanst.-A* **1987**, *39*, 305–313.
86. Paasche, E. Roles of nitrogen and phosphorus in coccolith formation in *Emiliania huxleyi* (Prymnesiophyceae). *Eur. J. Phycol.* **1998**, *33*, 33–42. [CrossRef]
87. Sheward, R.M.; Poulton, A.J.; Gibbs, S.J.; Daniels, C.J.; Bown, P.R. Physiology regulates the relationship between coccosphere geometry and growth phase in coccolithophores. *Biogeosciences* **2017**, *14*, 1493–1509. [CrossRef]
88. Brownlee, C.; Wheeler, G.L.; Taylor, A.R. Coccolithophore biomineralization: New questions, new answers. *Sem. Cell Devel. Biol.* **2015**, *46*, 11–16. [CrossRef]

89. Walker, C.E.; Heath, S.; Salmon, D.L.; Smirnoff, N.; Langer, G.; Taylor, A.R.; Brownlee, C.; Wheeler, G.L. An extracellular polysaccharide-rich organic layer contributes to organization of the coccosphere in coccolithophores. *Front. Mar. Sci.* **2018**, *5*, 306. [CrossRef]
90. Sviben, S.; Gal, A.; Hood, M.A.; Bertinetti, L.; Politi, Y.; Bennet, M.; Krishnamoorthy, P.; Schertel, A.; Wirth, R.; Sorrentino, A.; et al. A vacuole-like compartment concentrates a disordered calcium phase in a key coccolithophorid alga. *Nat. Com.* **2016**, *7*, 11228. [CrossRef] [PubMed]
91. Gal, A.; Sviben, S.; Wirth, R.; Schreiber, A.; Lassalle-Kaiser, B.; Faivre, D.; Scheffel, A. Trace-element incorporation into intracellular pools uncovers calcium-pathways in a coccolithophore. *Adv. Sci.* **2017**, *4*, 1700088. [CrossRef] [PubMed]
92. Pomar, L.; Hallock, P. Carbonate factories: A conundrum in sedimentary geology. *Earth-Sci. Rev.* **2008**, *87*, 134–169. [CrossRef]
93. Newell, N.D. Mass extinctions at the end of the Cretaceous Period. *Science* **1965**, *149*, 922–924. [CrossRef]
94. Keller, G.; Mateo, P.; Punekar, J.; Khozyem, H.; Gertsch, B.; Spangenberg, J.; Bitchong, A.M.; Adatte, T. Environmental Changes during the Cretaceous-Paleogene Mass Extinction and Paleocene-Eocene Thermal Maximum: Implications for the Anthropocene. *Gondwana Res.* **2018**, *56*, 69–89. [CrossRef]
95. Hallock, P. Fluctuations in the trophic resource continuum: A factor in global diversity cycles? *Paleoceanography* **1987**, *2*, 457–471. [CrossRef]
96. d'Halloy, J.-J. Observations sur un essai de carte géologique de la France, des Pays-Bas, et des contrées voisines [*Observations on a trial geological map of France, the Low Countries, and neighboring countries*]. *Ann. Des Mines* **1822**, *7*, 353–376.
97. Lear, C.H.; Rosenthal, Y.; Wright, J.D. The closing of a seaway: Ocean water masses and global climate change. *Earth Planet. Sci. Lett.* **2003**, *210*, 425–436. [CrossRef]
98. Adams, C.G.; Lee, D.E.; Rosen, B.R. Conflicting isotopic and biotic evidence for tropical sea-surface temperatures during the Tertiary. *Palaeogeog. Palaeoecol.* **1990**, *77*, 289–313. [CrossRef]
99. Stanley, S.M.; Hardie, L.A. Secular oscillations in the carbonate mineralogy of reef-building and sediment-producing organisms driven by tectonically forced shifts in seawater chemistry. *Palaeogeog. Palaeoecol.* **1998**, *144*, 3–19. [CrossRef]
100. Pearson, P.N.; Palmer, M.R. Atmospheric carbon dioxide concentrations over the past 60 million years. *Nature* **2000**, *406*, 695–699. [CrossRef] [PubMed]
101. Pochon, X.; Montoya-Burgos, J.I.; Stadelmann, B.; Pawlowski, J. Molecular phylogeny, evolutionary rates, and divergence timing of the symbiotic dinoflagellate genus *Symbiodinium*. *Mol. Phylogenet. Evol.* **2006**, *38*, 20–30. [CrossRef] [PubMed]
102. Wooldridge, S.A. Breakdown of the coral-algae symbiosis: Towards formalising a linkage between warm-water bleaching thresholds and the growth rate of the intracellular zooxanthellae. *Biogeosciences* **2013**, *10*, 1647–1658. [CrossRef]